Received: 21 October 2019 | Revised: 16 March 2020 | Accepted: 2 April 2020

DOI: 10.1002/ame2.12114

ORIGINAL ARTICLE

A segmental defect adaptation of the mouse closed femur fracture model for the analysis of severely impaired bone healing

Amandeep Kaur[1] | Subburaman Mohan[1,2,3] | Charles H. Rundle[1,2]

[1]Musculoskeletal Disease Center, Research Service (151), Jerry L. Pettis Memorial Veterans Administration Medical Center, Loma Linda, CA, USA

[2]Department of Medicine, Loma Linda University, Loma Linda, CA, USA

[3]Department of Orthopedic Surgery, Loma Linda University, Loma Linda, CA, USA

Correspondence
Charles H. Rundle, Musculoskeletal Disease Center, Research Service (151), Jerry L. Pettis Memorial Veterans Administration Medical Center, 11201 Benton St, Loma Linda, CA 92357, USA.
Email: charles.rundle@va.gov

Funding information
Loma Linda Veterans Association for Research and Education, Grant/Award Number: Seed Grant (to CR); US Department of Veterans Affairs, Grant/Award Number: Merit Review Award # 5 I01 BX002519-04 (to CR) and Senior Research Career Scientist Award (to SM)

Abstract

Objective: To better characterize nonunion endochondral bone healing and evaluate novel therapeutic approaches for critical size defect healing in clinically challenging bone repair, a segmental defect model of bone injury was adapted from the three-point bending closed fracture technique in the murine femur.

Methods: The mouse femur was surgically stabilized with an intramedullary threaded rod with plastic spacers and the defect adjusted to different sizes. Healing of the different defects was analyzed by radiology and histology to 8 weeks postsurgery. To determine whether this model was effective for evaluating the benefits of molecular therapy, BMP-2 was applied to the defect and healing then examined.

Results: Intramedullary spacers were effective in maintaining the defect. Callus bone formation was initiated but was arrested at defect sizes of 2.5 mm and above, with no more progress in callus bone development evident to 8 weeks healing. Cartilage development in a critical size defect attenuated very early in healing without bone development, in contrast to the closed femur fracture healing, where callus cartilage was replaced by bone. BMP-2 therapy promoted osteogenesis of the resident cells of the defect, but there was no further callus development to indicate that healing to pre-surgery bone structure was successful.

Conclusions: This segmental defect adaptation of the closed femur fracture model of murine bone repair severely impairs callus development and bone healing, reflecting a challenging bone injury. It is adjustable and can be compared to the closed fracture model to ascertain healing deficiencies and the efficacy of therapeutic approaches.

KEYWORDS

bone fractures, bone morphogenetic protein 2, intramedullary fracture fixation, ununited fractures

1 | INTRODUCTION

Several million bone fractures occur each year in the United States, resulting in a significant health and economic burden.[1] While fracture repair is routinely efficient, approximately 10% of bone fractures display severely impaired healing that often requires surgical interventions. In addition to the severity of the injury, physiological conditions related to the age and health of the individual can impair bone repair and result in nonunion bone healing.[2-5]

Endochondral bone repair proceeds through a highly ordered series of steps that regulate the development of diverse skeletal tissues that bridge the bone injury with a soft tissue callus that ossifies and remodels the bone to the pre-injury state.[6] Animal models of bone repair have provided considerable information on the molecular and cellular pathways of bone repair, and the closed three-point bending fracture model has been a valuable model for fracture studies in rodent subjects.[7] However, absent a compromising physiology such as age or disease, the closed rodent fracture model normally heals efficiently without intervention,[8] and its utility for investigations of impaired bone healing is limited. Because of the availability of genetically engineered strains, the mouse has become the research subject of choice for investigations of bone healing, even when species differences might complicate the translation to larger models and clinical conditions.[9,10] It is therefore still necessary to develop mouse models of bone repair that can be used to study severely impaired bone healing and evaluate its response to therapeutic applications.

Descriptions of mouse models of nonunion bone healing often emphasize adaptations of orthopedic surgical procedures that utilize various fixating apparatus to stabilize a segmental defect injury so that it does not heal and is therefore considered to be a critical size defect.[8] A fixator must resist axial, bending and torsional forces to maintain defect spacing and alignment. While greater interfragmentary strain benefits bone formation within small defects, it is negatively associated with bone formation within larger defects.[11] Axial forces tend to result in compression of the defect that might be interpreted as a healing fracture. Bending rigidity is a very critical component of the defect fixation and is the other major cause of fixator failure. Torsional rigidity is inversely proportional to the defect length and is less sensitive to the size of the defect than the bending strength. However, very rigid fixators that completely resist these forces can delay callus formation until eventual fixator failure.

Proper stabilization to maintain a defect also requires optimal alignment of the components of the apparatus within the bone, as the forces exerted on the apparatus by the femur are considerable and can cause its weakening and eventual failure. Common orthopedic fixators, whether internal or external, are often uniplanar and unilateral.[12] Interior plates can introduce stress shielding to one side of the bone, which can increase porosity and inhibit callus formation at least on one side of the bone. The result is often a model with asymmetric callus development or even stabilized to a degree where there is no identifiable periosteal response to injury that can identify the impaired stages of defect callus development. In this respect, they might be better suited for evaluating orthopedic scaffold implants, rather than characterizing critical size defect healing.[13] Cortical pin or screw diameters cannot exceed 30% of the bone diameter,[12] which requires very accurate placement and alignment to avoid loosening and failure of the stabilization but that can also be difficult in a small target such as the adult mouse femur. It is therefore necessary to develop reliable bone repair models that allow the identification of normal callus tissues that fail in nonunion healing, for the elucidation of the impairment and the development of therapeutic alternatives.

We therefore sought to develop an intramedullary surgical stabilization extrapolated from the well-characterized closed femur fracture model, but where endochondral bone healing that is very severely impaired or has proceeded to nonunion healing can be compared with the closed femur fracture callus.[14] Because intramembranous and endochondral bone formation during fracture healing is mediated by the periosteum,[15-18] the periosteum and developing callus must remain free from metal fixtures used to stabilize injury, so an intramedullary apparatus that is easily removable upon harvest with minimal damage to the periosteal tissues facilitates the subsequent analysis of healing by radiology and histology. Avoiding external fixtures[19] also minimizes infection during the prolonged healing times required for the analysis of serious bone injury healing. Additionally, this approach also allows for minor adjustments in the defect size to vary the severity of impaired healing for the investigation of bone repair.

2 | MATERIALS AND METHODS

2.1 | Animals

The protocol and procedures were reviewed and approved by the Institutional Animal Care and Use Committee in compliance with the US National Research Council's Guide for the Care and Use of Laboratory Animals, the US Public Health Service Policy on Humane Care and Use of Laboratory Animals, and Guide for the Care and Use of Laboratory Animals. Surgery was performed on male C57BL/6 mice at 12 to 14 weeks of age (Jackson Labs). The size of male mice facilitated the development of the procedure, but it is expected to be easily adaptable to female mice, as is the case with the closed femur fracture model.

2.2 | Segmental defect surgery

2.2.1 | Defect apparatus

This technique relies on a screw mechanism provided by a threaded intramedullary rod that is screwed into the trochanter and the condyle with plastic tubing secured to the proximal and distal ends to fix the defect spacing at the midshaft. Briefly, the surgical procedure uses a #303 stainless-steel all-thread stud (0.5 mm major diameter, Unified Miniature 6.3 threads/mm; APEX) as the threaded rod that

is sheathed in polytetrafluoroethylene (PFTE) and polyimide plastic tubing and inserted in the intramedullary canal to maintain defect the spacing and alignment of the proximal and distal portions of the femur (Figure 1A). If the desired outside diameter PTFE tubing is not commercially available, it is possible to use a heat source to stretch 1.0 mm diameter #24 PTFE tubing over a 0.5 mm diameter metal rod or needle to reduce its outside diameter to fit inside the intramedullary cavity, while maintaining the inside diameter to accommodate the threaded rod. Polyimide tubing (0.0195″ inside diameter) at the center of the threaded rod at the defect site improves bending rigidity while minimizing the intramedullary space occupied by this apparatus, which avoids contact with the cortical periosteum at the edges of the defect and permits some motion during healing. We have also found that the polyimide tubing eases threading of rod through the PFTE tubing, and facilitates this adjustment of the distance between the proximal and distal PTFE tubing after insertion into the intramedullary space; the position of this tubing on the threaded rod determines the spacing, and its grip on the threads is critical for maintaining the defect spacing (arrows in Figure 1A,B). The apparatus is conveniently and aseptically manipulated during procedures using pipette tips that are threaded onto either end of the rod for handling (left in Figure 1A).

2.2.2 | Femoral segmental defect surgery

Anesthesia consists of 3% isoflurane delivered with 0.5 L/min oxygen through a nonrebreathing Bains circuit. The surgical site is shaved and treated with "Betadine". The femur is approached through a skin incision in the lateral aspect of the hindlimb. The biceps femoris and vastus lateralis muscle groups are separated to provide the exposure of the femur from the trochanter to the condyle. A 0.5 mm diameter dental burr is used to bisect the femoral midshaft under irrigation. The defect apparatus is then inserted into the distal femoral intramedullary space through the defect and threaded in anterograde fashion through a hole prepared with a 30 gauge needle in the intramedullary aspect of the condyle (Figure 1B). It is threaded through the condyle enough to reduce the length protruding from the defect and allow the proximal end to then be inserted into the intramedullary space of the femur proximal to the defect. When the proximal and distal ends of the defect are sufficiently aligned, the rod is secured at the proximal end by threading it into the intramedullary trochanter.

Defect size is then adjusted by holding each half of the femur apart while threading the rod through the condyle to increase the defect size and out of the condyle to decrease the defect size. Once the desired size is achieved the pipette tip-rod combination is threaded into the condyle to secure the apparatus. The rod and tip are both cut flush at the condyle; the pipette tip remaining on the rod in the condyle acts as an interference pin assisting the anchoring of the apparatus in the condylar bone (Figure 1B). Minor protrusions of intramedullary stabilization into the joint do not affect ambulation. The muscle groups and the skin are closed. The result is

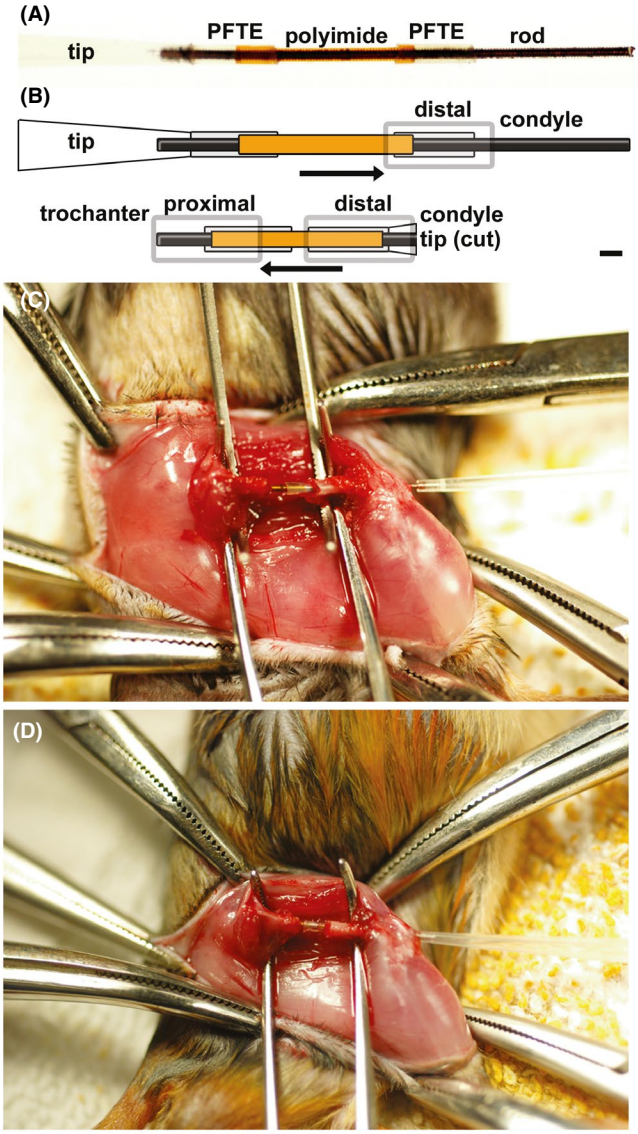

FIGURE 1 Segmental defect surgery. A, The intramedullary apparatus consists of a 0.5 mm diameter threaded rod fitted with polyimide (yellow) and PFTE (clear) tubing. A laboratory pipette tip (right) is threaded over the end simply to assist with aseptic handling. B, A diagrammatic illustration of the apparatus before insertion (upper) and in final form within the intramedullary space (lower). During intramedullary insertion from the defect toward the condyle, the PFTE tubing is forced over the polyimide tubing toward the center of the rod, indicated by the arrows. The pipette tip is switched to the condylar end of the apparatus to assist with threading the rod into the trochanter and defect size is adjusted before it is finally cut with the rod flush at the condyle. C and D, Once positioned in the intramedullary space and threaded into the trochanter, the final defect size can be adjusted: C, to more than 3.5 mm. D, to 2.5 mm, used in these studies. Scale bar = 1 mm

an intramedullary rod (a) threaded into the trochanter at the proximal end, (b) anchored at the condyle by the combination rod and tip interference pin, (c) and secured at its proximal and distal ends by intramedullary plastic tubing threaded securely to the rod at each end of the intramedullary space that (d) increases its bending strength

and prevents compression of the defect, but that can be adjusted from larger (Figure 1C) to smaller sizes (Figure 1D). Analgesia consists of buprenorphine at a 60 μg/kg dosage provided subcutaneously during surgery and every 12 hours thereafter for at least 2 days postsurgery. Other than the routine postsurgical discomfort, normal ambulation is regained within the first week of healing.

Because this surgical approach was adapted from the rodent closed femur fracture model, the histology of segmental defects that displayed severely impaired healing were compared with that of the rodent closed femur fracture model.[20] Callus development in this model has been well characterized and can offer insights into tissue development impaired by the defect.

To determine whether such a model of impaired bone healing is feasible for the evaluation of therapeutic efficacy, we compared healing of the segmental defect with and without the applications of bone morphogenetic protein (BMP)-2, a standard osteogenic growth factor. The defect was prepared with a viscous "Hydrogel" formulation ("Tegaderm" Hydrogel Wound Filler, 3M) to maintain viscosity and retention of the therapy, and subsequently wrapped in a layer of sterile "Surgicel" dressing (Ethicon). BMP-2 was injected at 25 μg/mL in percutaneous injections of 10 μL to the lateral aspect of the defect at 2 healing times well characterized in closed fracture healing for when its effects were expected to be most beneficial: 4 days postsurgery, when inflammation had subsided and intramembranous bone formation initiated, and 7 days postsurgery, during the early stages of chondrogenesis and endochondral bone formation. Control defects received the BMP-2 neutral-saline solvent. Harvest and analysis were performed as for the segmental defects without no BMP-2 intervention.

2.2.3 | Analysis of segmental defect healing

Table 1 summarizes the numbers of individuals in each group that underwent the radiologic analysis of the healing of the different sized defects examined, the histomorphometric comparison of callus cartilage development between the segmental defect and the closed fracture models, and the evaluation of the therapeutic efficacy of the osteogenic BMP-2 growth factor in the segmental defect.

Healing of the segmental defect was monitored weekly for 8 weeks in vivo by X-ray imaging. Upon tissue harvest at 8 weeks postsurgery, the apparatus was removed and micro-CT analysis using a Scanco *Viva*-CT 40 system (Scanco USA) characterized the development of the bony defect callus. The resolution of this instrument is 10.4 μm. The entire defect was contoured for analysis and included the cortical bone at the edges of the defect to account for new intramembranous bone formation that initiates fracture callus bone formation.[17] This region of interest was then segmented using a two-threshold approach that resolves the lower density woven bone of the developing callus (250–570 mg/cm^3) from the higher density native cortical bone (570–1000 mg/cm^3). These thresholds were determined using the bone density preview function of the Scanco analysis software that provided the optimum discrimination of each bone density when compared visually to the grayscale image.

Histology of the defect callus was compared with the closed fracture callus histology in paraffin-embedded sections to identify defect tissues that displayed impaired development during healing. Tissue harvests from each model were performed at 1 and 4 weeks postsurgery. Multiple sections from 2.5 mm defects and closed fracture calluses were examined from the center of the callus, as identified by the intramedullary space. Chondrogenesis is critical to endochondral bone formation; cartilage was identified by Safranin-Orange staining and quantified by histomorphometry using "ImagePro" software (Media Cybernetics) by a blinded observer experienced in rodent fracture surgery and histology. Photomicrographs were obtained using an Olympus BX60 microscope and DP72 camera.

Statistical analysis was performed by analysis of variance with Tukey posthoc testing for micro-CT and histology analysis, and Student's *t*-test for the analysis of BMP-2 therapy. Results were considered significant at $P < .05$.

3 | RESULTS

3.1 | Analysis of the defect by radiology

X-ray analysis is presented immediately following surgery (Figure 2A-C), and at healing intervals of 4 weeks (Figure 2D-F)

TABLE 1 Summary of segmental defect analysis

Objective	Analysis approach	Healing	Surgical injury	Group size	Therapy
Defect healing	X-ray, micro-CT	4, 8 wk	1.5 mm defect	6	None
			2.5 mm defect	13	
			3.0 mm defect	7	
Callus cartilage	Histomorphometry	1 wk	Closed fracture	7	None
			2.5 mm defect	5	
		4 wk	Closed fracture	4	
			2.5 mm defect	6	
Therapy efficacy	X-ray, micro-CT	8 wk	2.5 mm defect	7	BMP-2
			2.5 mm defect	4	Saline control

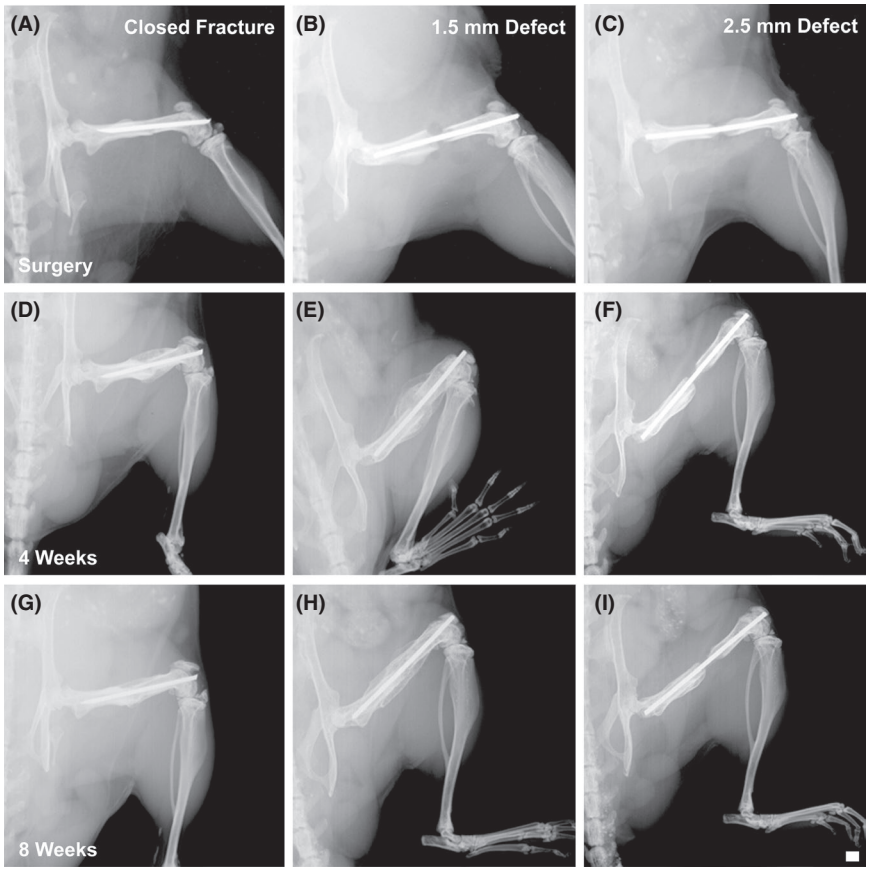

FIGURE 2 Analysis of bone healing by *in vivo* X-ray examination of the femur. A-C, Surgery. D-F, 4 weeks healing. G-I, 8 wk healing. A, D, G, Closed fracture. B, E, H. 1.5 mm segmental defect. C, F, I, 2.5 mm segmental defect. Scale bar = 1 mm

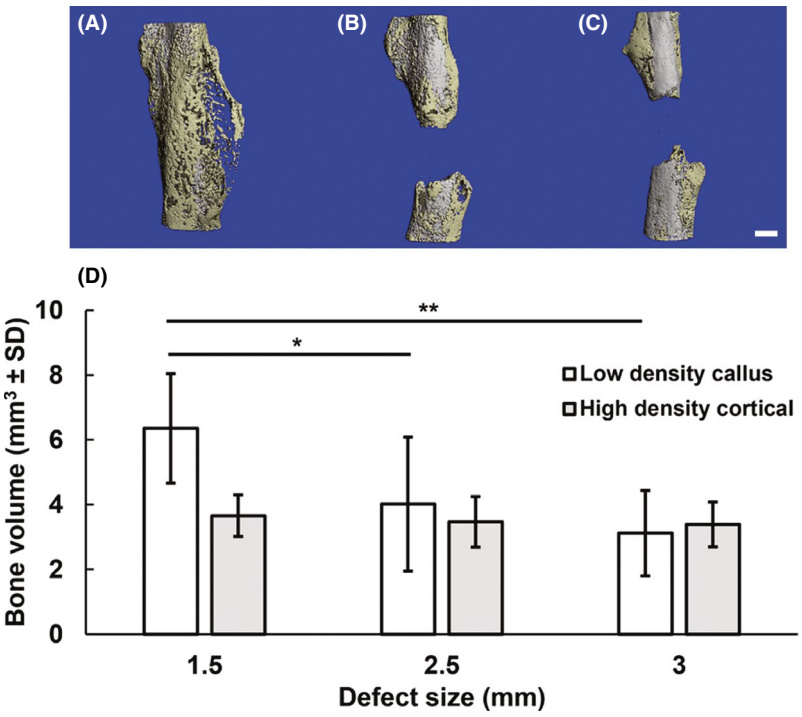

FIGURE 3 Micro-CT analysis of the healing of segmental defects at 8 weeks postsurgery. A, 1.5 mm. B, 2.5 mm. C, 3 mm. D, Bone volume was compared for low density woven bone of the fracture callus and higher density cortical bone in group sizes of 6 to 13 mice. $^{*}P < .05$, $^{**}P < .01$. Scale bar = 1 mm

and 8 weeks (Figure 2G-I), and illustrates that the size of the defect was associated with the degree of callus bone formation, but that further hard callus development had ceased by 8 weeks postsurgery. The closed fracture developed a bony callus that achieved bony union by 4 weeks and was remodeling by 8 weeks (Figure 2A,D,G). In the 1.5 mm defect, a bony callus developed and appeared to be remodeling by 8 weeks (Figure 2B,E,H). However, the larger bony callus observed at 8 weeks suggests that its

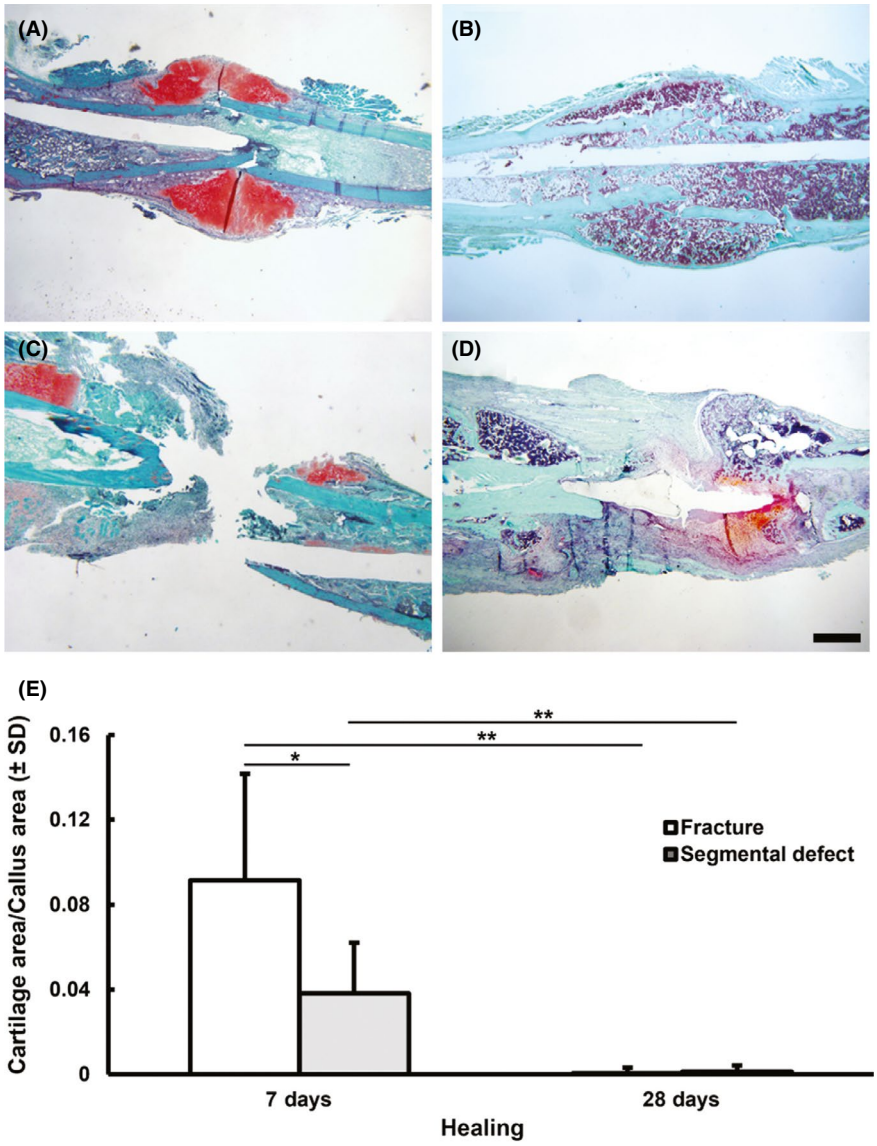

FIGURE 4 Comparison of closed fracture and segmental defect histology by Safranin-O stains of the fracture or defect cartilage. A, B, Closed fracture. C, D, Segmental defect. A, C, 1 week postsurgery. B, D, 4 weeks postsurgery. E, The cartilage area per callus area was quantified for group sizes of 4 to 7 mice. *P < .05, **P < .01. Scale bar = 1 mm

healing was much more delayed than in the closed fracture callus. In contrast, the 2.5 mm defect failed to develop any radio-dense tissues within the defect, even by 8 weeks healing, indicating that bone formation was severely impaired and that this size defect appears to be a critical size (Figure 2C,F,I). Thus, the defect size determined the degree of bony callus development.

The development of the bony defect callus was further characterized by micro-CT analysis of healing of 1.5, 2.5, and 3.0 mm segmental defects at 8 weeks postsurgery (Figure 3A-C, respectively). Comparisons of the different sized segmental defects confirmed the *in vivo* X-ray examination results of Figure 2. The 1.5 mm defect appeared to develop a bony callus and to undergo delayed healing (Figure 3A) similar to the 1.8 mm defect healing observed by the intramedullary pin/clip approach.[21] There was no bone evident within the 2.5 mm and 3.0 mm defects, although there was bone on the periosteal surfaces of the opposing cortices that was consistent with intramembranous fracture callus bone formation that had ceased and eventually adopted a rounded appearance characteristic of pseudoarthrosis (Figure 3B,C).

The bone volume (BV) of the callus was quantified using the two-threshold approach (Figure 3D). The reduced lower density callus BV in the 2.5 mm (4.0 ± 2.1 mm^3, P < .05) and 3.0 mm (3.1 ± 1.3 mm^3, P < .01) defects relative to the 1.5 mm defect (6.4 ± 1.7 mm^3) demonstrates that bone formation failed within those gaps, indicating that the 2.5 mm defect did indeed represent a critical size threshold for callus endochondral bone formation. This observation was confirmed in additional animals examined at this defect size (Table 1). The higher density bone consistent with callus remodeling to cortical bone was not significantly different for any size defect, suggesting that even when capable of bone formation, healing was still impaired in the 1.5 mm defect. We have not pursued defect callus development beyond 8 weeks to determine whether remodeling can be completed in this defect. These results suggest that healing was at least very severely delayed and possibly approaching nonunion.

3.2 | Analysis of defect histology

A comparison of the fracture and defect cartilage established that a soft fracture callus did form by 1 week healing, but when compared with closed fracture chondrogenesis and cartilage development (Figure 4A) there was a significant reduction in cartilage abundance in the 2.5 mm segmental defect (Figure 4B). By 4 weeks healing, closed fracture healing had achieved bony union (Figure 4C), but fibrous tissues persisted between the proximal and distal ends of the segmental defect. Hard callus also remained on the periosteal surface at the ends of the injured bone, but the cartilage appeared to have attenuated (Figure 4D). Thus, histological analyses supported the micro-CT analysis that while a periosteal response initiated intramembranous bone formation, the reduced cartilage abundance in the defect at 1 week healing (0.04 ± 0.02 %, $P < .05$) relative to the closed fracture (0.09 ± 0.05%, Figure 4E) indicates that endochondral bone healing response was very severely delayed, if not completely inhibited by the time of bony union in the closed fracture model. The cartilage in both models was negligible at 4 weeks ($P < .01$, Figure 4E), but was apparently attenuated without bony union of the tissues in the 2.5 mm defect.

3.3 | Evaluation of BMP-2 therapy

The BMP-2 therapy was injected percutaneously postsurgery to the defect that was prepared at surgery with "Hydrogel" (Figure 5A) wrapped in a "Surgicel" barrier (Figure 5B). An examination at 8 weeks healing revealed that BMP-2 promoted bone formation within the defect tissue relative to the saline control (Figure 5C,D), but by 8 weeks postsurgery the low density BV produced by BMP-2 persisted within the defect (5.4 ± 2.1 mm^3 vs 3.05 ± 0.8 mm^3 control, $P < .05$, Figure 5E) where it apparently failed to remodel to higher density cortical bone and instead appeared heterotopic (Figure 5D).

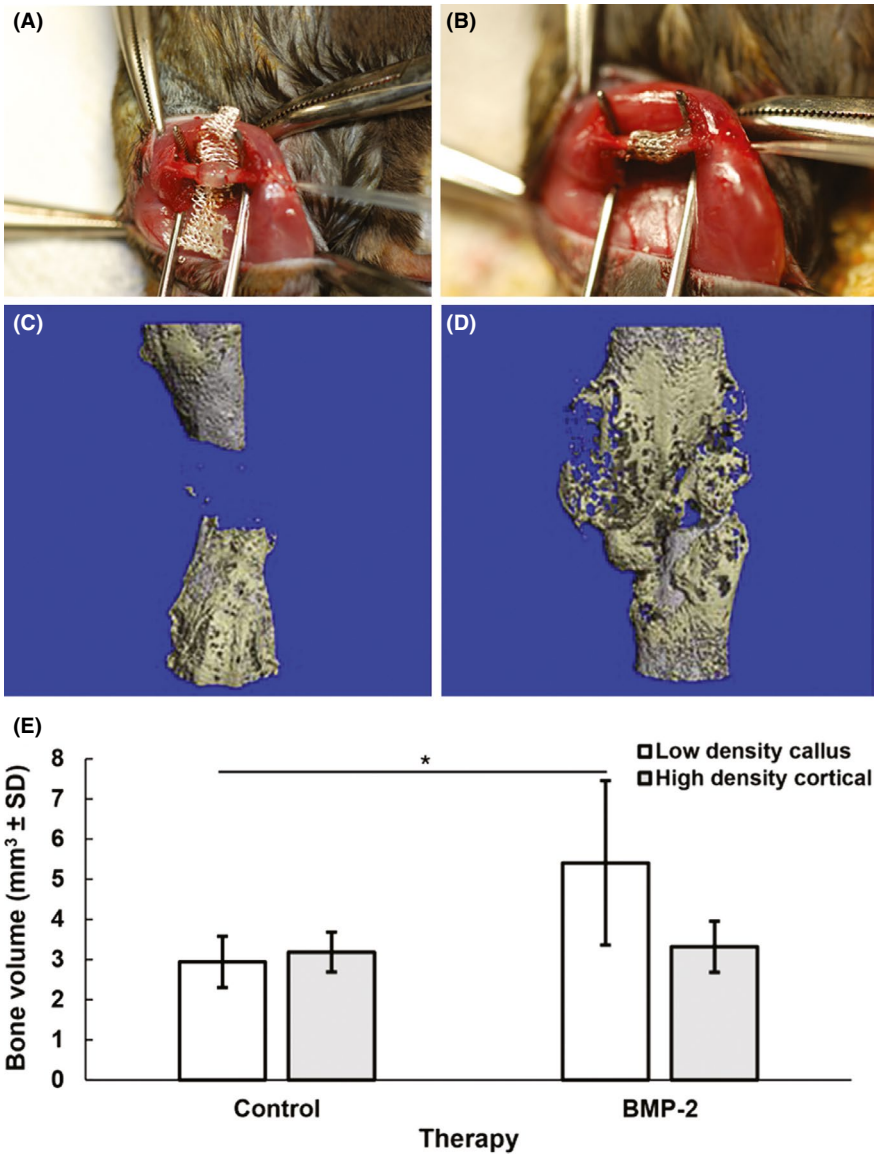

FIGURE 5 Segmental defect therapy. A, "Hydrogel" was placed in the defect during surgery and wrapped in a surgical mesh. B, A 2.5 mm segmental defect is shown prepared for postsurgical injection of BMP-2 therapy. Micro-CT analysis of BMP-2-mediated bone formation was performed at 8 weeks postsurgery. C, Control. D, BMP-2 therapy. E, Bone volume was compared for low density fracture callus woven bone and higher density remodeled callus and cortical bone for group sizes of 4 to 7 mice. *$P < .05$. Scale bar = 1 mm

4 | DISCUSSION

Unless patient healing is compromised by age or a physiological condition that impairs normal bone repair, simple closed endochondral bone fractures heal well enough that intervention is unnecessary. Here, we describe a procedure that can be used to investigate critical size defect healing and evaluate molecular therapy in a clinically challenging model of bone repair. Its intramedullary stabilization (Figure 1A,B) is similar to the commonly used closed fracture rodent model of bone repair, which allows comparisons to the closed femur fracture model callus development to identify and characterize the stages of healing that are affected by a large bone injury such as the segmental defect. It is similar in concept but simpler than the locking femur nail "LockingMouseNail",[22] although it avoids the rigid cortical pin fixation of this and other approaches,[21] as well as the pin-collar design that uses a defect-long collar to stabilize the defect.[23] Its limitations on animal size are those of the closed fracture three-point bending technique.

This surgical approach uses a simple apparatus fabricated from easily available components, easily steam-sterilized for aseptic surgery and disposable upon tissue harvest. Defect spacing is maintained by the incorporation of plastic tubing spacers securely threaded to each end of the intramedullary rod to prevent the compression or total collapse of the defect. It avoids screw and plate attachment to the injured bone, and there are no externally exposed components to allow for exposure of the defect to environmental contaminants and infection. An infrequent bending or breaking of the rod can be avoided by the choice of materials. Because the rigidity of the intramedullary pin is proportional to the fourth power of its radius,[12] a very small increase in its diameter will greatly increase the bending strength, an important consideration for the forces exerted on the femur. Increased endosteal contact of an intramedullary fixator also increases its load-sharing and reduces failures, although it impairs the endosteal circulation.[24] Very importantly, the apparatus is easy to remove from the femur upon harvest. It is simply threaded out through the condyle, avoiding damage to the defect tissues during the removal of pins, screws, clips or plates that stabilize other segmental defect approaches.[8,25] If any plastic components are retained in the intramedullary space, they can be excluded from micro-CT analysis by segmentation and are easily sectioned with the tissue for histology procedures, facilitating the analysis.

Comparisons of this defect model with the closed fracture model have indicated that it always results in severely delayed fracture repair and proceeds to nonunion healing characteristic of a critical size defect, at least by the 8 week healing times that we examined. Surgery was designed to produce a segmental defect in the femoral midshaft of approximately 2.5 mm, an injury that does not normally heal. However, it also offers the opportunity to adjust the size of the defect to evaluate healing in defects in which the severity of the injury is minimal, such as that of the closed fracture, to 3.0 mm, which at 20% of the length of adult mouse femur is quite severe. When the radiology is analyzed by X-ray examination, closed fracture healing appears to complete bony union and is progressing through remodeling, while segmental defects of increasing sizes impair callus bone formation, which is especially evident in the 2.5 mm defect (Figure 2C,F,I).

Histological examination compared closed fracture and segmental critical size defect healing and revealed that a soft defect callus formed and chondrogenesis initiated, but cartilage formation was much less abundant at 1 week than in the closed fracture, attenuating thereafter. Segmental defect healing assumed a nonunion appearance by 4 weeks postprocedure, when fibrous tissues persist between the ends of the defect (Figure 4D). The micro-CT and histological analyses confirmed that the endochondral bone formation response in the segmental defect model was very severely delayed, if not completely arrested. We conclude that endochondral bone formation in the segmental defect is impaired at an early stage of healing.

Among the different aspects of bone repair that might contribute to the impairment observed in the segmental defect, the complete absence of a periosteum within the defect is an important concern.[15,16] This investigation could be approached by (a) the application of exogenous cells with bone forming potential on a matrix, such as mesenchymal stem cells on a collagen sponge, or (b) by simply reducing the defect size in this model to reduce the distance between periosteal surfaces on either side of the injury to determine at what distance healing can proceed. We have demonstrated the latter approach for a 1.5 mm size defect by radiological approaches, and a histological examination of a less severe impairment might identify and more accurately characterize the obstacle to bone formation when compared with this defect or the closed fracture.

Despite a significant loss of periosteum in the segmental defect model, a direct *in vivo* injection of BMP-2 protein was effective in promoting osteogenesis within the injury (Figure 5D). In this respect it appeared very similar to the severely delayed healing of the 1.5 mm defect callus without therapy (Figure 3D). However, while bony tissue formed within the defect, we did not observe any further development of a bony callus from 2 to 8 weeks of healing in the *in vivo* X-ray examinations, indicating that a normal fracture callus did not develop beyond 2 weeks. The reason for impaired healing in response to therapy remains to be investigated, but callus remodeling is an obvious candidate for further study. Bone formation appears functional, but the bone does not appear to develop into a normal fracture callus, even at a time that is twice the normal 4 weeks required for bony union in the closed fracture. It is therefore difficult to conclude that a linear examination of healing radiology or histology beyond the 8 weeks of the fracture-defect comparison in Figure 5 would reveal any further development of a callus toward eventual bony union of the injury and subsequent remodeling to pre-injury bone appearance. Rather, it is probable that as observed in segmental defect healing without therapeutic intervention (Figure 3), the periosteum that is missing is necessary to mediate normal callus development,[16,17] and in its absence the bone formation produced by the nonperiosteal resident cells of the defect in response to BMP-2 therapy is heterotopic.[26]

This model appears similar to the distraction and implant approach used in the first step of the induced membrane approach developed by Masquelet for bone regeneration in large defects.[27,28] However, in our study the apparatus is intramedullary, designed to maintain a specified defect size without interfering with the periosteal healing response in the mouse, an easily available and genetically defined research subject. It is not therapeutic. Importantly, it can be adjusted to permit different degrees of callus formation similar to the closed fracture model (Figure 2) that facilitate the investigation of molecular and cellular regulation of bone repair for the eventual application to clinically challenging bone repair. If periosteal cells are required for repair of the defect, this question could be pursued most easily in this model again by reducing the size of the defect to a distance threshold where enough of periosteal surface remains that normal, nonheterotopic callus bone develops and remodels for study. Nevertheless, this model is still effective for the assessment of the therapeutic efficacy of protein therapy strategies to augment different metabolic processes of bone repair in more clinically challenging bone injuries. It presumably would also be effective for the evaluation of gene therapy and material implants in promoting defect repair.

In conclusion, this murine segmental defect model of bone injury is a valuable approximation of a more challenging bone healing than the closed femoral fracture model. It permits comparisons with closed fracture healing that might identify the impairment in critical size defect healing and facilitate the development of therapeutic applications for clinically challenging bone repair.

ACKNOWLEDGMENTS

The authors thank Nancy Lowen for assistance with the histology. This work was supported by a Seed Grant from the Loma Linda Veterans Association for Research and Education and by Merit Review Award # 5 I01 BX002519-04 (CR) from the United States (U.S.) Department of Veterans Affairs Biomedical Research and Development Program. SM is the recipient of a Senior Research Career Scientist Award from the U.S. Department of Veterans Affairs. The contents do not represent the views of the U.S. Department of Veterans Affairs or the United States Government.

CONFLICT OF INTEREST

None.

AUTHOR CONTRIBUTIONS

AK contributed to the design of the study, the acquisition and interpretation of the data and the drafting of the manuscript. SM contributed to the analysis and interpretation of the data and to critical revisions of the manuscript. CR contributed to the conception and design of the study, the acquisition, analysis and interpretation of the data, and the drafting and critical revisions of the manuscript. All authors approved the final version of the manuscript.

ORCID

Charles H. Rundle https://orcid.org/0000-0003-4691-8143

REFERENCES

1. Buza JA III, Einhorn T. Bone healing in 2016. *Clin Cases Miner Bone Metab*. 2016;13(2):101–105.
2. Claes L, Recknagel S, Ignatius A. Fracture healing under healthy and inflammatory conditions. *Nat Rev Rheumatol*. 2012;8(3):133–143.
3. Clark D, Nakamura M, Miclau T, Marcucio R. Effects of aging on fracture healing. *Curr Osteoporos Rep*. 2017;15(6):601–608.
4. Hak DJ. The biology of fracture healing in osteoporosis and in the presence of anti-osteoporotic drugs. *Injury*. 2018;49(8):1461–1465.
5. Jiao H, Xiao E, Graves DT. Diabetes and its effect on bone and fracture healing. *Curr Osteoporos Rep*. 2015;13(5):327–335.
6. Einhorn TA, Gerstenfeld LC. Fracture healing: mechanisms and interventions. *Nat Rev Rheumatol*. 2015;11(1):45–54.
7. De Giacomo A, Morgan EF, Gerstenfeld LC. Generation of closed transverse fractures in small animals. *Methods Mol Biol*. 2014;1130:35–44.
8. Garcia P, Histing T, Holstein JH, et al. Rodent animal models of delayed bone healing and non-union formation: A comprehensive review. *Eur Cell Mater*. 2013;26:1–12; discussion 12–14.
9. Haffner-Luntzer M, Hankenson KD, Ignatius A, et al. Review of animal models of comorbidities in fracture-healing research. *J Orthop Res*. 2019;37(12):2491–2498.
10. Hadjiargyrou M, O'Keefe RJ. The convergence of fracture repair and stem cells: Interplay of genes, aging, environmental factors and disease. *J Bone Miner Res*. 2014;29(11):2307–2322.
11. Yamaji T, Ando K, Wolf S, Augat P, Claes L. The effect of micromovement on callus formation. *J Orthop Sci*. 2001;6(6):571–575.
12. Hasselman CT, Gruen GS. Principles of operative fracture stabilization and fixation. In: Fitzgerald RH, Kaufer H, Malkani AL, eds. *Orthopaedics*, 1st edn. St. Louis, MO: Mosby; 2002:228–238.
13. de Misquita MR, Bentini R, Goncalves F. The performance of bone tissue engineering scaffolds in in vivo animal models: a systematic review. *J Biomater Appl*. 2016;31(5):625–636.
14. Reichert JC, Saifzadeh S, Wullschleger ME, et al. The challenge of establishing preclinical models for segmental bone defect research. *Biomaterials*. 2009;30(12):2149–2163.
15. Arnsdorf EJ, Jones LM, Carter DR, Jacobs CR. The periosteum as a cellular source for functional tissue engineering. *Tissue Eng Part A*. 2009;15(9):2637–2642.
16. Duchamp de Lageneste O, Julien A, Abou-Khalil R, et al. Periosteum contains skeletal stem cells with high bone regenerative potential controlled by periostin. *Nat Commun*. 2018;9(1);773.
17. Debnath S, Yallowitz AR, McCormick J, et al. Discovery of a periosteal stem cell mediating intramembranous bone formation. *Nature*. 2018;562(7725):133–139.
18. Wang T, Zhang X, Bikle DD. Osteogenic differentiation of periosteal cells during fracture healing. *J Cell Physiol*. 2017;232(5):913–921.
19. Cheung KM, Kaluarachi K, Andrew G, Lu W, Chan D, Cheah KS. An externally fixed femoral fracture model for mice. *J Orthop Res*. 2003;21(4):685–690.
20. Bonnarens F, Einhorn TA. Production of a standard closed fracture in laboratory animal bone. *J Orthop Res*. 1984;2(1):97–101.
21. Garcia P, Holstein JH, Maier S, et al. Development of a reliable non-union model in mice. *J Surg Res*. 2008;147(1):84–91.
22. Garcia P, Herwerth S, Matthys R, et al. The lockingmousenail–a new implant for standardized stable osteosynthesis in mice. *J Surg Res*. 2011;169(2):220–226.
23. Clough BH, McCarley MR, Gregory CA. A simple critical-sized femoral defect model in mice. *J Vis Exp*. 2015;(97). https://doi.org/10.3791/52368
24. Olerud S, Stromberg L. Intramedullary reaming and nailing: its early effects on cortical bone vascularization. *Orthopedics*. 1986;9(9):1204–1208.
25. Manassero M, Decambron A, Huu Thong BT, Viateau V, Bensidhoum M, Petite H. Establishment of a segmental femoral critical-size

defect model in mice stabilized by plate osteosynthesis. *J Vis Exp*. 2016;(116). https://doi.org/10.3791/52940
26. Wang L, Tower RJ, Chandra A, et al. Periosteal mesenchymal progenitor dysfunction and extraskeletally-derived fibrosis contribute to atrophic fracture nonunion. *J Bone Miner Res*. 2019;34(3):520–532.
27. Giannoudis PV, Faour O, Goff T, Kanakaris N, Dimitriou R. Masquelet technique for the treatment of bone defects: tips-tricks and future directions. *Injury*. 2011;42(6):591–598.
28. Masquelet A, Kanakaris NK, Obert L, Stafford P, Giannoudis PV. Bone repair using the masquelet technique. *J Bone Joint Surg Am*. 2019;101(11):1024–1036.

How to cite this article: Kaur A, Mohan S, Rundle CH. A segmental defect adaptation of the mouse closed femur fracture model for the analysis of severely impaired bone healing. *Animal Model Exp Med*. 2020;3:130–139. https://doi.org/10.1002/ame2.12114